Electron Paramagnetic Resonance Studies of Spin-Labeled Fatty Acid Binding Sites in *Candida Rugosa* Lipases

Cristina Otero,* Ricardo Castro, and Javier Soria

Instituto de Catálisis y Petroleoquímica, CSIC, Campus Universitario, Cantoblanco, 28049 Madrid, Spain

Horia Caldararu

Romanian Academy, Institute of Physical Chemistry "I.G. Murgulescu", Splaiul Independentei 202, 77208 Bucharest, Romania

Received: April 7, 1998; In Final Form: June 19, 1998

Electron paramagnetic resonance (EPR) spectroscopy has been used to characterize the binding of spin-labeled fatty acids (SLFA) to two isolipases (lipases A and B) from *Candida rugosa*. The spectra of the bound species obtained with 5-doxyl and 16-doxyl stearic acids (5-DSA and 16-DSA) at a low molar ratio of fatty acid to lipase (0.15/1) have been analyzed using slow motion EPR simulations. Analysis of the EPR parameters extracted from the simulations (rotational diffusion coefficients, $R_{||}$, $R_{\perp}$, and R) supports the existence of a tunnel in the enzyme which imposes constraints on the motion of the SLFA. These constraints depend on both the nature of the lipase (there is higher mobility of the label in lipase A than in lipase B) and the position of the label (the mobility at C-16 of the SLFA is higher than at C-5 for lipase A). With respect to both the C-5 and C-16 positions of the bound SLFA, the polarities of both isolipases (measured from the isotropic hyperfine splitting, A_o, in the low temperature spectra) are essentially the same. This result implies nearly identical polarities at the substrate binding region of these enzymes. However, the polarity at the C-5 position is greater than that at C-16. The polarity data lead one to the conclusion that differences in the activities of *C. rugosa* isolipases are not a consequence of differences in the polarity of the protein binding region. The lower specific activity of lipase A relative to that of lipase B for the hydrolysis of triacylglycerols has been interpreted in terms of the mobility and binding data for the two SLFA's. Binding studies (Scatchard analysis) involving different molar ratios of fatty acid to lipase (0.1/1−5/1) for 5-DSA and 16-DSA indicate the presence of four interdependent binding sites for these substrates in the isolipases from *C. rugosa*. For both isolipases, the association constants are of the order of 10^4, a value which is characteristic of specific ligand−protein interactions. The binding constant for isolipase A is higher than that for B. In terms of the cooperative character of the binding, the interactions of these fatty acid analogues with *C. rugosa* isolipases are consistent with a conformational rearrangement of the hydrophobic pocket of the protein.

Introduction

Lipases (E.C. 3.1.1.3) are triacylglycerol hydrolases.[1] The mechanism of the hydrolysis consists of several steps and remains to be fully elucidated, but a proposed mechanism has been extrapolated from that proposed for serine proteases.[2,3] The final step involves the release of a carboxylic acid. In nearly anhydrous organic media, fatty acids are also substrates of lipases in esterification reactions. Lipase activity is greatly increased at the lipid/water interface.[4,5] This interfacial activation is related to conformational changes in the lipase molecule involving displacement of a loop (or "flap") which covers the active site.[6−9] However, there is a need for information concerning the role of the lipid recognition site in catalysis by lipases. Characterization of the lipid binding sites of different lipases is required to achieve a better understanding of the mechanism of action of lipases.

Various fungal species (for example, *Candida rugosa* and *Geotricun candidum*) produce lipase isoenzymes differing in biochemical properties, in substrate specificity and in their lipase-encoding genes.[10−15] Variability within lipases from a particular *fungus* has been related to the ability of the microorganism to adapt to different nutrients in various physiological conditions. Thus, comparative studies of different lipases of the same family might be useful in efforts to decipher the mechanism used by lipases to recognize and distinguish different substrates.

Different laboratories have purified the major isolipase from *C. rugosa*[16−18] (lipase sequence termed *LIP*1[11,12]). In the Instituto de Catálisis-CSIC we have isolated and purified a minor isolipase (termed lipase A) from *C. rugosa*[13,18] (lipase sequence termed *LIP*3[15]). Lipase A differs significantly from other isolipases in activity and specificity for substrates and in its great ability to establish hydrophobic interactions both in affinity chromatography[18] and at the interface of reverse micelles.[14] The remaining *C. rugosa* isolipases (lipase B) are very similar in their biochemical and enzymatic properties.[18] The open and closed conformations of the major isospecies have been crystallized.[19,20]

In an effort to understand aspects of the mechanism of substrate−enzyme interactions in lipases in general and to

* To whom correspondence should be addressed. C.O.: e-mail, cotero@icp.csic.es; telephone, 34−91−5854805; fax, 34−91−5854760.

10.1021/jp981781h CCC: $15.00
Published on Web 09/25/1998

structurally distinguish isolipase A from the other isolipases of *C. rugosa* in particular, we have undertaken an EPR study of the interactions of lipases A and B with a ligand closely related to the product of hydrolysis of esters, a long chain fatty acid. As a model compound for this study, we have employed stearic acid, which was labeled with a doxyl group at two different sites (5- and 16-).

This spin labeling technique has been widely used for the characterization of fatty acid binding to serum albumin,[21−31] β-lactoglobulin,[32] and α-lactalbumin.[33] Characterization involves measuring the equilibrium binding constants, probing the binding sites, and identifying the rate and the nature of the motion of the bound fatty acid.

The present study had as its major objectives provision of more quantitative information on the nature (polarity, steric hindrance, etc.) and strength of the binding sites of fatty acids in lipases via measurements of appropriate EPR parameters and by simulation of the corresponding EPR spectra of the bound label. In pursuit of these objectives, this study has taken advantage of the similarities and differences (especially in hydrophobicity and substrate specificity) in the biochemical and structural properties of the two isoenzymes A and B from *C. rugosa*. This system of isoenzymes has been exploited to obtain a consistent, more general picture of fatty acid−lipase interactions. There is a scarcity of data relative to fatty acid−lipase binding. To our knowledge, the present study is the first which uses a spin-labeling technique to obtain such information. The dynamic description of binding phenomena in aqueous solution reported here may complement the static information obtained in studies of the crystal structure of lipases.[19,20]

Experimental Section

Materials. *C. rugosa* lipase Type VII, *p*-nitrophenyl butyrate (pNPB), and spin-labeled stearic acid (SLFA)—2-(3-carboxypropyl)-4,4-dimethyl-2-tridecyl-3-oxazolidinyloxy (5-doxyl stearic acid, 5-DSA), 2-(14-carboxytetradecyl)-2-ethyl-4,4-dimethyl-3-oxazolidinyloxy (16-doxyl stearic acid, 16-DSA)—were purchased from Sigma, Ltd. (St. Louis, MO).

Purification of Crude Lipase. Purification to achieve homogeneity was carried out as previously described.[18] Purified lipases A (one isolipase) and B (four isospecies including the major isolipase, which was present in the highest proportion) were lyophilized and stored at −20 °C until used. The specific activities of lipases A and B for pNPB were 5×10^{-3} and 5×10^{-4} M s^{-1}/mg, respectively. The hydrolytic activities of these lipases were measured by following the accumulation of *p*-nitrophenol in a Kontron 930 UVIKON spectrophotometer equipped with thermostated cells at 30 ± 0.1 °C. In all cases, the reaction mixtures consisted of 1.39 mM pNPB in 0.1 M sodium phosphate buffer, pH 7.2, containing 3% (v/v) acetonitrile. The absorbance was measured at the isosbestic point of the nitrophenol/nitrophenolate couple (346 nm; molar extinction coefficient 4800 M^{-1} cm^{-1}). The initial rate was obtained in less than 2 min.

Calibration Curves and Formation of SLFA−Lipase Complexes. Stock solutions of SLFA in acetonitrile were prepared and stored at 4 °C. Different dilutions of the stock solution were used to obtain calibration plots for free SLFA. In all cases, the solution of SLFA in 0.1 M sodium phosphate buffer, pH 7.2, also contained 2% (v/v) acetonitrile. SLFA−lipase complexes were prepared as follows. The exact amounts of SLFA in acetonitrile were added to a sample tube containing a 0.1 M sodium phosphate buffer solution, pH 7.2, of the lipase to produce the required SLFA/lipase ratio and a final acetonitrile concentration of 2% (v/v). The solution was stirred for 15 min at 20 °C. Solutions with SLFA/lipase ratios from 0.1 to 5 were prepared by varying the concentration of the label at a constant concentration (2×10^{-4} M) of lipase. SLFA−lipase complexes in a buffer−glycerol (1/1 w/w) solution with a SLFA−lipase ratio of 0.15/1 were prepared in similar fashion for measurements at low temperature (220 K).

We have previously demonstrated that the presence of 2% (v/v) acetonitrile does not produce any significant conformational changes in either lipases (0% decrease in their α-helix contents[34]). A higher concentration of acetonitrile (3% (v/v)) is typically used for determination of the lipolytic activities of these lipases without any adverse effect on their intrinsic properties.[14,18]

Both the solutions containing the SLFA−lipase complexes and samples for the calibration curves were transferred to thin-wall calibrated capillaries and measured under rigorously identical instrumental conditions. The equilibrium distribution of free and bound SLFA for the different SLFA/lipase ratios was determined by measuring the height of the $M = -1$ (high-field component of the nitrogen hyperfine splitting) line which is associated with free SLFA in solution. This peak height was compared to standard curves of the peak height (I) vs known concentration of SLFA in buffer solution (containing 2% w/w acetonitrile). The bound SLFA was estimated as the difference between the total and free SLFA.

The dependencies of I vs concentration of SLFA were similar to those found by Rehfeld et al.[27] and by Perkins et al.[29] for the same spin labels. Most of the points of the Scatchard plots were measured in the region where the concentration of free SLFA was below the critical micellar concentration (cmc) ($\sim 5 \times 10^{-5}$ M and $\sim 1 \times 10^{-4}$ M for 5-DSA and 16-DSA, respectively) of the corresponding label. However, concentration values above the cmc were measured for the last two to three points in the Scatchard plots of 5-DSA. In these cases, the observed peak amplitudes, I, were higher than those present in the calibration curves. This behavior is most probably a result of increased solubilization of SLFA in the presence of the enzyme, which itself causes a substantial increase in the corresponding cmc. In these cases, the concentration of the free SLFA was evaluated by assuming that the straight portion of the calibration curve can be extrapolated above the cmc. This assumption appears to be valid since the last experimental points for the Scatchard plots fit the theoretical curve (see eq 1) very well, and the number of binding sites determined with 5-DSA is the same as that found with 16-DSA (see below). To avoid problems of this type, some authors have used relatively high concentrations of organic solvents (e.g., ethanol) for increasing the cmc,[33] after proving that the protein of interest is not affected by this procedure. In our case, this approach could not be used, because the addition of the required amount of organic solvents (short chain alcohols) would denature the isolipases.[35]

EPR Measurements and Spectra Analysis. EPR spectra were recorded at 293 K on a 200 D-SRC Bruker instrument with 100 kHz modulation using X-band frequency. Spectra were recorded at 100 G magnetic field scan ranges, by employing 20 mW microwave power and a 1 G (peak-to-peak) modulation amplitude. A higher modulation amplitude (1.5 G) was used for recording the "bound" spectra. The spectra at low temperature (220 K) were recorded using the variable temperature attachments of the instrument (Model ER-4111 VT).

The spectra of the bound SLFA were also analyzed in terms of $2A_{||}$, the distance between the outermost peaks from the 100 G scans.[22,27,29,31]

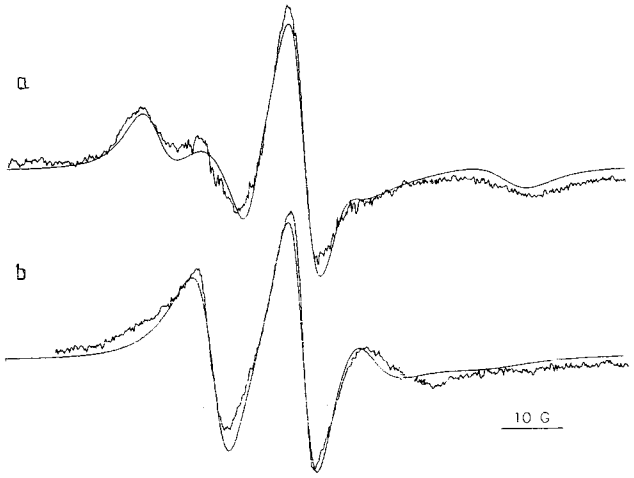

Figure 1. EPR spectra at 293 K and computer simulations of (a) 5-DSA and (b) 16-DSA bound to lipase A (SLFA/lipase ratio of 0.15/1). Experimental settings were the same for both labels.

For the simulation of the 293 K spectra, usually four scans were accumulated. The spectrum of the bound label was obtained after subtraction of the free SLFA spectrum. Computer simulations of experimental EPR spectra were performed using an IBM-compatible 486 personal computer, using the program of Freed et al.[36] for slow motion. The rotational correlation time, τ_R, is defined as $\tau_R = (6R)^{-1}$ with $R = (R_{||}R_{\perp})^{1/2}$, where $R_{||}$ and $R_{\perp}$ are the rotational diffusion coefficients about the axes parallel and perpendicular to the diffusion tensor. For the low-temperature spectra in the rigid-limit region, simulations were performed using a program of G. P. Lozos, B. M. Hoffman, and C. G. Franz,[37] modified by J. M. Logan.

Analysis of Binding Isotherms. The analytical procedure described by Schreier and Schimmel[38] for the case of dependent sites (cooperative binding) was employed to study the binding interactions. The equation of Scatchard[39,40] for the case of a class of interacting sites (protein cooperativity) is

$$n/c = (NK^{\alpha}c^{\alpha-1})/(1 + K^{\alpha}c^{\alpha}) \quad (1)$$

where N is the number of interacting sites, K is the association constant, α is the interaction exponent (cooperativity parameter), n is the molar ratio of bound ligand/protein, and c is the concentration of free ligand. When the cooperativity is positive, the Scatchard curve has a positive curvature. The n intercept at $n/c \rightarrow 0$ ($c \rightarrow \infty$) gives N. Values of K and α were obtained from plots of ln c vs ln($N/n - 1$) which give straight lines:

$$\ln c = -1/\alpha \ln(N/n - 1) - \ln K$$

Results

Dynamics (Mobility) of Bound SLFA. To compare the behavior of lipases A and B toward the two spin labels, their EPR spectra have been analyzed at a low molar ratio of SLFA to lipase (0.15), where most of the label is bound to the enzyme and the "bound" spectrum is least affected by the presence of free labels in solution. In this case, on average only a single ligand molecule is bound to the enzyme (see the Scatchard analysis below). Figures 1 and 2 show the room temperature (293 K) EPR spectra of 5-DSA and 16-DSA bound to each of the two lipases. The spectra depicted in these figures are the result of accumulation of several scans for each sample, followed by subtraction of the appropriate spectrum of the corresponding DSA label in buffer solution. The spectra correspond to the slow motion region.[36] Comparison of the features of the spectra

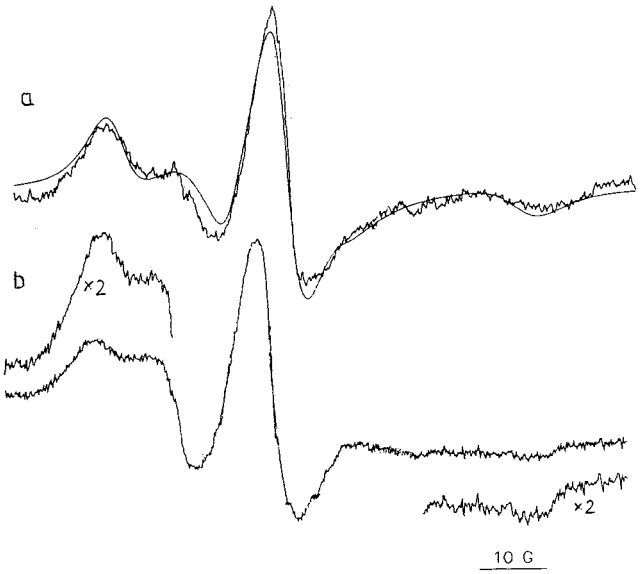

Figure 2. EPR spectra at 293 K and computer simulations of (a) 5-DSA and (b) 16-DSA bound to lipase B (SLFA/lipase ratio of 0.15/1). Experimental settings were the same for both labels.

in Figures 1 and 2, together with the measured value of the spectral parameter, $2A_{||}$, permits one to clearly distinguish between the mobilities of the two SLFA in the two lipases. Thus, for lipase A: $2A_{||} = 61.8 \pm 0.4$ G for 5-DSA and there are no $2A_{||}$ features for 16-DSA. For lipase B: $2A_{||} = 65.2 \pm 0.4$ G for 5-DSA and $2A_{||} = 63.0 \pm 1.0$ G for 16-DSA. Contribution of the overall tumbling of the enzyme to the SLFA spectral parameters may be ruled out, since the size of the enzyme is 50 Å × 42 Å × 33 Å,[20,41] and the threshold value for the radius of the enzyme above which this contribution is outside the range of detectability by EPR measurements is ~25 Å.[42−44] It is well-known that there are two possible contributions to the $2A_{||}$ value in such cases—the polarity of the surroundings of the nitroxide moiety and the motion thereof (with correlation times in the 10^{-9}−10^{-7} s range). The $2A_{||}$ value may also be affected by Heisenberg spin exchange (at frequencies approaching those of the nitrogen hyperfine interactions). Analysis of the $2A_{zz}$ values indicates that contribution of the polarity may be ruled out as a factor by which one can distinguish between the $2A_{||}$ values of the same label in lipases A and B. The $2A_{zz}$ value—the rigid limit value—is a measure of polarity only, because at low temperature (220 K) motion of the nitroxide fragment practically ceases. Thus, examination of spectra recorded at 220 K (Figure 3) reveals that although the $2A_{zz}$ values for each label in the two lipases are almost identical (68.5 ± 0.2 G and 69.0 ± 0.2 G for 5-DSA in lipases A and B, respectively, and 65.4 ± 0.2 G and 65.6 ± 0.2 G for 16-DSA, in lipases A and B, respectively), the corresponding $2A_{||}$ values are substantially different. The nitroxide moieties of the two labels have higher mobilities in lipase A than in lipase B. This conclusion is also semiquantitatively reflected in the Δ ($\Delta = 2A_{zz} - 2A_{||}$) values. This parameter is relatively insensitive to changes in polarity and intramolecular Heisenberg spin exchange. Hence, it provides a more reliable measure of the label mobility.[45] The Δ value of 6.7 ± 0.6 G for 5-DSA in lipase A relative to the value of 3.8 ± 0.6 G in lipase B indicates a much higher mobility of the nitroxide moiety in the former enzyme than in the latter. Although the Δ value for 16-DSA in lipase A could not be evaluated, it is evident from examination of the shape of its spectrum in Figure 1 that the motion of the 5-DSA nitroxide moiety in lipase A is more restricted than that of the

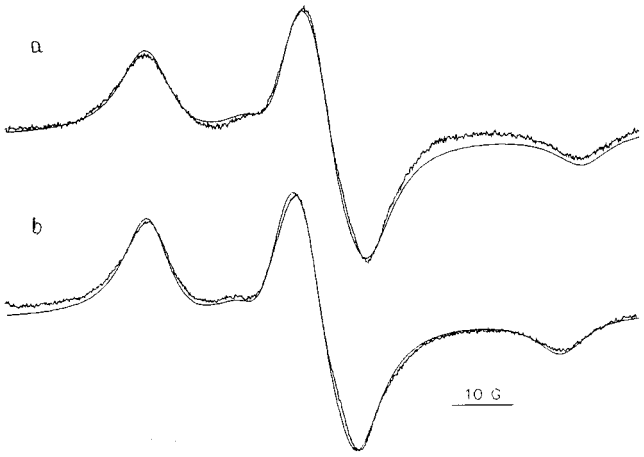

Figure 3. EPR spectra at 220 K and computer simulations of (a) 5-DSA and (b) 16-DSA bound to lipase A (SLFA/lipase ratio of 0.15/1) in 1/1 (w/w) buffer/glycerol mixture; simulation carried out using the following parameters: (a) $A_{xx} = 5.5$ G, $A_{yy} = 5.5$ G, $A_{zz} = 34.25$ G, $g_{xx} = 2.0084$, $g_{yy} = 2.0055$, and $g_{zz} = 2.0021$; (b) $A_{xx} = 5.5$ G, $A_{yy} = 5.5$ G, $A_{zz} = 32.7$ G, $g_{xx} = 2.0084$, $g_{yy} = 2.0055$, and $g_{zz} = 2.0021$.

16-DSA nitroxide moiety. In the case of lipase B, the values of the Δ parameter were 3.8 ± 0.6 G and 2.6 ± 1.2 G for 5-DSA and 16-DSA, respectively.

Regarding the polarities of the microenvironments encountered by the nitroxide moieties of the two spin labels in lipases A and B, the rigid limit values of $2A_{zz}$ clearly indicate (i) nearly identical polarities for the same label in the two lipases and (ii) different polarities for 5-DSA and 16-DSA in the same enzyme. Since the parameter which actually characterizes the polarity changes is the isotropic value of the hyperfine splitting tensor **A**,[46] $A_o = 1/3(A_{xx} + A_{yy} + A_{zz})$, this parameter will be discussed below after simultation of the spectra.

To elucidate in more quantitative terms the nature and the rate of label motion in the two lipases, simulations[36] of the spectra corresponding to a molar ratio of SLFA/lipase of 0.15/1 (Figures 1 and 2) were carried out. Because the simulations are not sufficiently sensitive to distinguish differences between spectra of different SLFA/lipase molar ratios, the other ratios were characterized by the $2A_{||}$ parameter (Figure 4). In these cases, even after accumulation of more spectra, the $2A_{||}$ value could not be measured above a certain SLFA/lipase molar ratio because the spectrum of the bound label was obscured by that of the free species. The observed increase in $2A_{||}$ at very low molar ratios of SLFA to lipase is followed by a decrease in this parameter as the SLFA/lipase molar ratio is increased further. It is difficult to distinguish which factor (polarity, rate of motion, or nitroxide−nitroxide interactions) makes the predominant contribution to this parameter when additional lipase sites are populated by bound SLFA (see the discussion below concerning the determination of the number of binding sites). It seems reasonable to attribute the decreasing portion of the plot to a decrease in the polarity of the microenvironment of the doxyl group and/or an increase in its mobility.

The computer simulations of the spectra in Figures 1 and 2 require the components of the **A** and **g** tensors.[36] These components were evaluated from the corresponding spectra of the SLFA/lipase A complexes obtained at 220 K (Figure 3). Rigid limit spectra of the corresponding SLFA/lipase B complexes are almost identical, showing very small differences in the measured A_{zz} values. A_{zz} and g_{zz} could be measured directly from the experimental spectra, but the other components of the **A** and **g** tensors were determined from the best simulations[37] (Figure 3). Very good agreement is observed between the

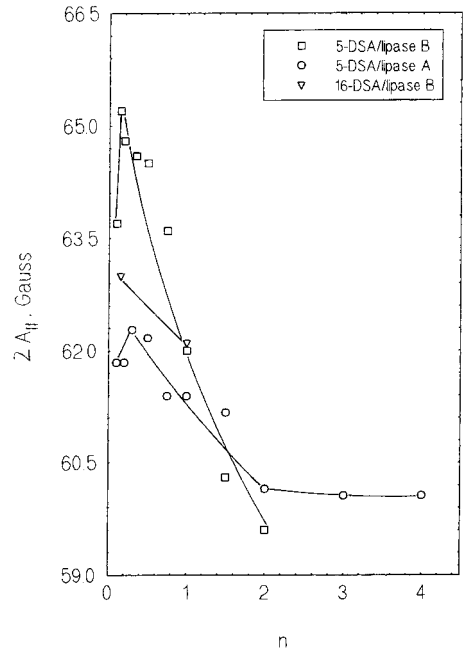

Figure 4. Variation of $2A_{||}$ as a function of the SLFA/lipase ratio.

TABLE 1: Components of the A Tensor from Simulation of the Rigid Limit Spectra (220 K) of SLFA Bound in an SLFA/Lipase Complex[a]

lipase	SLFA	A_{xx} (G)	A_{yy} (G)	A_{zz}[b] (G)	A_o (G)
A	5-DSA	5.5	5.5	34.25	15.1
A	16-DSA	5.5	5.5	32.70	14.6
B	5-DSA	5.5	5.5	34.50	15.2
B	16-DSA	5.5	5.5	32.80	14.6

[a] The molar ratio of SLFA to lipase was 0.15. [b] The experimental errors in measuring the corresponding A_{zz} values are given in the text.

experimental and simulated spectra (Figure 3). The best fit values of the **g** tensor components are $g_{xx} = 2.0084$, $g_{yy} = 2.0055$, and $g_{zz} = 2.0021$ (this value has been experimentally measured with an error of ± 0.0001) for all rigid limit spectra. The components of the **A** tensor based on the best simulations are given in Table 1. The values in Table 1 indicate that the component most affected by the polarity is A_{zz}. The isotropic values of the hyperfine tensor **A**, A_o, in Table 1, clearly show that both in lipase A and lipase B, the nitroxide group in the labeled 5-DSA finds itself in much higher polarity environment ($A_o = 15.1$ G) than does this group in 16-DSA ($A_o = 14.6$ G). The former value is closer to values which characterize media in which hydrogen bonding to the nitroxide group is significant (e.g., in water where $A_o = 15.6$ G[47]). The latter value is closer to that observed in very hydrophobic media (*e.g.*, in *n*-decane where $A_o = 13.9$ G[47]).

The values of the components of the **A** and **g** tensors given in Table 1 are used as input parameters for the program of Schneider and Freed[36] which was used to simulate the spectra shown in Figures 1 and 2. The best correlations between the experimental and simulated spectra (Figures 1 and 2) were achieved using a Brownian diffusion model which included diffusion tilt angles, and in which for all cases the motion around the long chain of the SLFA (the *z* axis) is more rapid than in the plane perpendicular to the *z* axis. No improvement was noted if the same diffusion model was employed for rotation around the other axes. However, for the experimental spectrum of the 16-DSA/lipase A complex, which is in a faster region (Figure 1), essentially identical simulations could be obtained

TABLE 2: Rotational Correlation Times (τ) and Rotational Diffusion Coefficients (R) Obtained from Computer Simulation of Spectra (293 K) of SLFA Bound in the SLFA/Lipase Complex[a]

lipase	SLFA	$R_\perp$ (s^{-1})	$\tau_\perp$ (ns)	$R_\parallel$ (s^{-1})	$\tau_\parallel$ (ns)	R (s^{-1})	τ_R (ns)
A[b]	5-DSA	1×10^7	16.7	8×10^7	2.1	2.8×10^7	6.0
A[c]	16-DSA	4.5×10^7	3.7	8×10^7	2.1	6.0×10^7	2.8
B[d]	5-DSA	4×10^6	41.6	8×10^7	2.1	1.8×10^7	9.3

[a] The ratio of SLFA to lipase was 0.15. [b] Input parameters: $A_{xx} = 5.5$ G, $A_{yy} = 5.5$ G, $A_{zz} = 34.25$ G, $g_{xx} = 2.0084$, $g_{yy} = 2.0055$, and $g_{zz} = 2.0021$; tilt angle, $\phi = 30°$; natural line width, $T_2^{-1*} = 1$ G. [c] As in footnote *b*, except $A_{zz} = 32.7$ G, $\phi = 20°$, and $T_2^{-1*} = 1$ G. [d] As in footnote *b*, except $A_{zz} = 34.5$ G and $T_2^{-1*} = 2$ G.

using a constant $R_\perp$ value (4.5×10^7 s^{-1}) but various $R_\parallel$ values within the range from 4.5×10^7 s^{-1} (tilt angle $\phi = 0°$) to 1×10^8 s^{-1} ($\phi = 20°$). For $R_\parallel > 1 \times 10^8$ s^{-1}, the simulated spectra became very sensitive to changes in this parameter. In this case, we opted to employ simulation with a tilt angle in order to maintain consistency of interpretation. For the spectra corresponding to regions of slower motion (5-DSA/lipase A and 5-DSA/lipase B), the closeness of the best fit of the simulations was more sensitive to changes in the diffusion parameters (in these cases, changes of ± 0.2 in the significant figures of the diffusion coefficients (Table 2) lead to noticeable differences in the shape of the simulated spectra). In the case of the 16-DSA/lipase B complex, the different simulation trials failed to achieve fairly good fit of the features of the experimental spectrum (Figure 2b). In this case, even the uncertainty in the measurement of the $2A_\parallel$ value is higher than that in the other cases. Hence, the simulation has not been presented here. The low value of the binding constant for the lipase B/16-DSA complex (see below) seems to be the responsible for the difficulty of achieving a good fit of the experimental spectrum.

The values of the rotational diffusion coefficients, $R_\parallel$, $R_\perp$, and R, as well as the corresponding rotational correlation times, $\tau_\parallel$, $\tau_\perp$, τ, obtained from the optimal simulations are shown in Table 2. The following observations should be noted: (i) the overall rate of motion, R, of 5-DSA is higher in lipase A than in lipase B, and in lipase A, the rate of motion is higher for 16-DSA than for 5-DSA; (ii) at the same rate of motion around the long axis of the fatty acid (the z axis) ($R_\parallel = 8 \times 10^7$ s^{-1}), the rate of motion for 5-DSA in a perpendicular plane is much higher in lipase A ($R_\perp = 1 \times 10^7$ s^{-1}) than in lipase B ($R_\perp = 4 \times 10^6$ s^{-1}); (iii) at the same rate of motion around the z axis in lipase A, the rate of motion in a perpendicular plane is slower for 5-DSA ($R_\perp = 1 \times 10^7$ s^{-1}) than for 16-DSA ($R_\perp = 4.5 \times 10^7$ s^{-1}).

The quantitative estimates of the parameters determined from the simulations are consistent with the semiquantitative evaluations of the mobilities of the two SLFA labels in the two lipases estimated from the Δ values discussed above. This parallelism supports the use of Δ values to evaluate the mobilities of spin labels in various media[45] when simulation is not possible. However, although this approach provides crude estimates of relative mobilities, it fails to provide adequate details concerning the nature of the motion of the label.

Binding of SLFA to Lipases. Number of Binding Sites and Binding Constants. Typical EPR spectra obtained for different 5-DSA/lipase A and 16-DSA/lipase A ratios are given in Figures 5 and 6, respectively. Examination of these spectra reveals that as the ratio of acid to enzyme increases, the relative height of the free peak also increases. This behavior was also observed with lipase B (not shown).

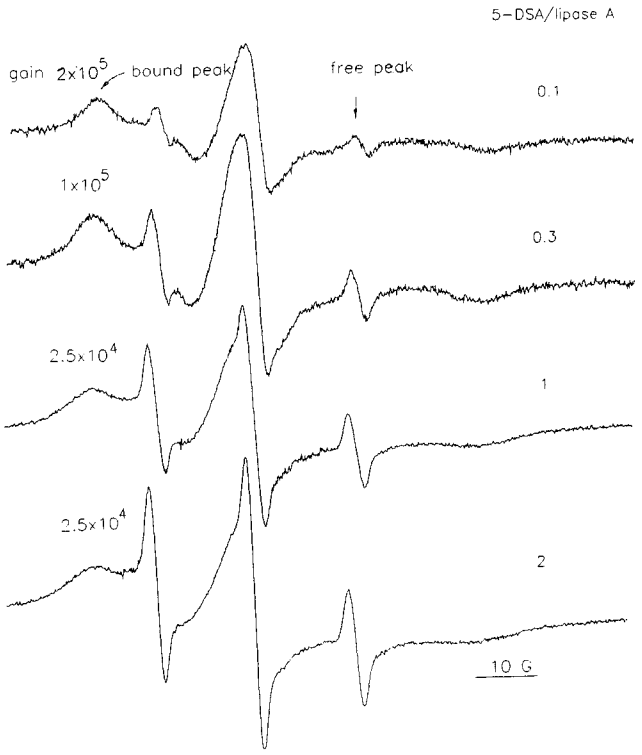

Figure 5. EPR spectra of 5-DSA for various SLFA/lipase A ratios at 293 K. Experimental settings were the same for all samples, except for the indicated receiver gain. The peak corresponding to free SLFA is indicated on the spectrum.

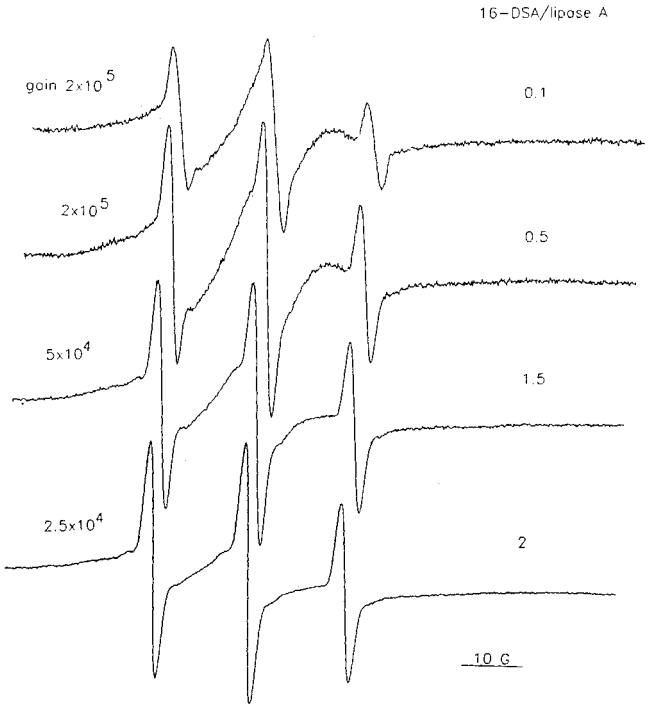

Figure 6. EPR spectra of 16-DSA at 293 K for various SLFA/lipase A ratios. Experimental settings were the same for all samples, except for the indicated receiver gain. The peak corresponding to the free SLFA is indicated on the spectrum.

The SLFA/lipase binding isotherms are presented as plots of n vs c and as Scatchard plots (n/c vs n) in Figures 7 and 8, respectively. The experimental data are represented by circles and squares in these figures. The values of parameters of eq 1 (K, N, and α) which best fit the experimental data are given in Table 3. The corresponding theoretical curves are also shown

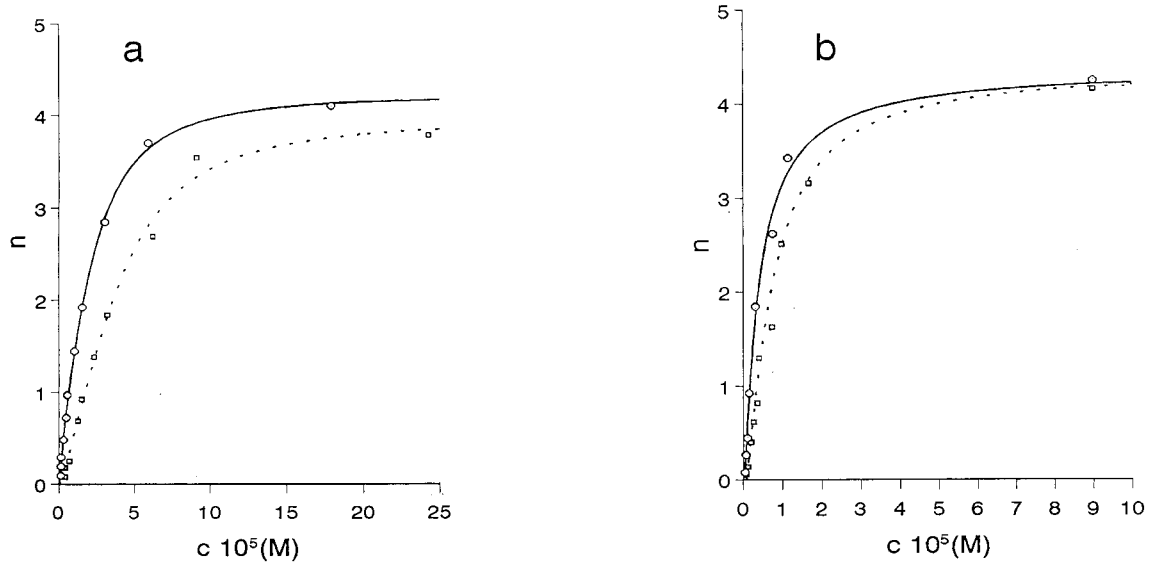

Figure 7. Binding isotherms for (a) 5-DSA and (b) 16-DSA bound to isolipases A (solid line) and B (dotted line).

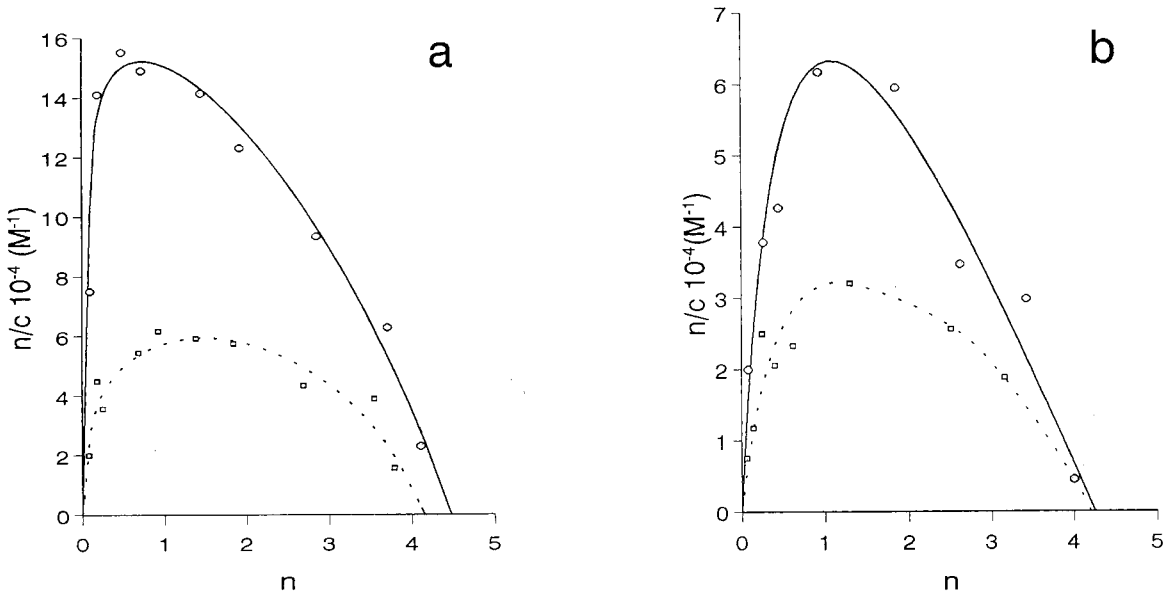

Figure 8. Scatchard plots of (a) 5-DSA and (b) 16-DSA bound to isolipases A (solid line) and B (dotted line).

TABLE 3: Parameters for SLFA Binding to Lipases

lipase	SLFA	*K*	*N*	α
A	5-DSA	5.3×10^4	4	1.2
A	16-DSA	2.3×10^4	4	1.5
B	5-DSA	2.7×10^4	4	1.5
B	16-DSA	1.2×10^4	4	1.7

in Figures 7 and 8. Inspection of Figure 8 indicates that (i) the occurrence of maxima in all the plots—bell-shaped curves—is evidence of cooperativity,[38] irrespective of the nature of the lipase and the SLFA, (ii) the binding of each SLFA is different in the two isoenzymes, (iii) in both lipases, the binding of 5-DSA is stronger than that of 16-DSA.

The Scatchard analysis demonstrates that all isolipases from these *fungi* have four interdependent binding sites for spin-labeled fatty acids. According to the value of α, the binding is cooperative positive. The order of magnitude of the values of the apparent association constant, *K*, corresponds to specific binding. The binding constants are more than twice as high for lipase A as for lipase B, and these constants depend on the label (5-DSA or 16-DSA) employed.

Discussion

Binding Studies at a Low Molar Ratio of SLFA to Lipase. Interpretation of all the information obtained from the EPR data at a low ratio of SLFA to lipase (0.15/1), together with the accepted model for the active site of lipases,[1] permits one to obtain a crude picture of the binding site(s) for the labeled fatty acids. These sites are thought to be potentially active for both polar and hydrophobic interactions. Since the polar interactions are stronger than the hydrophobic ones, the carboxylic group of the fatty acid can be imagined as being directed toward a fixed, polar site in the enzyme. This statement is supported by the fact that high values of the association constants were found for both lipases (see below). These values are indicative of specific ligand−protein interactions. X-ray studies[48] actually indicate that the carboxylic group of the acid interacts with the polar region of the binding pocket.

The higher polarity at the 5-position relative to that at the 16-position of the SLFA could be a consequence of the fact that the amino acid residues surrounding the 5-position in both lipase A and B have higher intrinsic polarities than those surrounding the 16-position. Consequently hydrophobic inter-

actions are more likely to occur at the latter position. The fact that, at both positions 5 and 16, one encounters nearly identical polarities in lipase A and lipase B (see Table 1 and the above discussion) supports the hypothesis that the binding site is the same in both enzymes.

The flexibility of the SLFA in the two lipases (see the dynamic parameters in Table 2) may be analyzed in terms of steric hindrance around the doxyl fragment. Thus, the very low, near rigid limit, values of $R_\perp$ and the relatively high values of $R_\parallel$ for both bound SLFAs in the two lipases (Table 2) indicate that rotational diffusion around the axis perpendicular to the hydrocarbon chain of the fatty acid is greatly hindered. Consequently, the motion of the SLFA seems to occur in a narrow tunnel. This finding may be correlated with data for crystal structures. The crystal structures of the major *C. rugosa* lipase−inhibitor complexes may be identified with a long, narrow, hydrophobic tunnel in which the fatty acyl chain is bound.[48] The tunnel which binds the acid moiety interacting with the catalytic *Ser* group projects itself toward the middle of the protein.[48]

The fact that the mobilities are different for the same SLFA in the two lipases, as well as for the two SLFAs in the same lipase indicates that there are differences in the steric hindrance encountered by the nitroxide moieties within said channel. From this point of view and from the relative values of the dynamic parameters (Table 2), a model which permits one to distinguish between the two lipases emerges: (i) a lower steric constraint is sensed by the label fragment in lipase A than in lipase B, at distances of both 4- and 15-bond lengths, respectively, from the site where binding of the carboxylate moiety occurs; (ii) in lipase A the steric hindrance at the 5-position of the fatty acid chain is greater than that at the 16-position. The variation of the mobility of the spin label of the acid bound to lipases A and B could be a consequence of differences in the amino acids forming the corresponding tunnel. The differences in structure lead to differences in steric hindrance in this region and/or to differences in nature of the interactions between the amino acids and the fatty acid. Analysis of the restricted number of amino acids most likely to be involved in the interaction with the substrate molecule for the major lipase (*LIP1*) and for lipase A (*LIP3*)[15] revealed that 10 of those amino acids are different in the two lipases. In particular, more than 50% of the differences in amino acids correspond to more hydrophobic species in *LIP3*. Because of this fact, the higher mobility of the ligand in this isospecies compared to that in lipase B seems to rule out greater hydrophobic interactions between isoform A and the ligand.

The variation in the polarity of the environment of doxyl along the chain length of the acid herein reported is in good agreement with the description of the tunnel of the major lipase obtained from crystallographic studies.[48] The first six atoms of the acid chain run above the helix following the nucleophile elbow, while the chain atoms C12−C17 fill the arm of the tunnel establishing van der Waals contacts with several amino acids of the protein.[46] Consequently, the increase in polarity associated with closer proximity of the doxyl group to the carboxylic group of the acid indicates that the labeled (doxyl) fatty acid is oriented in the tunnel of these lipases in a manner similar to that of natural (unlabeled) fatty acids under physiological conditions. Moreover, the nearly identical polarities around the nitroxide label for a given spin-labeled acid (5-DSA or 16-DSA) in the family of *C. rugosa* lipases imply that the polarities at the active site will be nearly identical. Therefore, the variations in substrate specificity[18] within this family of lipases are not associated with differences in the polarity of the binding site.

Changes in $2A_\parallel$ produced by increasing the SLFA concentration (Figure 4) indicates that once the first acid molecule is bound, additional binding sites in the binding pocket of the lipase are subsequently occupied. Since the structural data for crystallized lipase−inhibitor complexes indicate a second tunnel in the binding pocket,[48] the observed changes support the hypothesis that, as a result of subsequent occupation, the pocket undergoes a conformational rearrangement, which agrees with the cooperativity of the binding (see below).

Binding Studies at Different Molar Ratios of SLFA to Lipase. Differences in the Scatchard plots (Figures 7 and 8) and, accordingly, the different binding constants for 5-DSA and 16-DSA in the same lipase (Table 3) are a consequence of the influence of the second polar (doxyl) group, specifically its relative position, on the SLFA/lipase interaction. Hence, the nitroxide group and its specific position on the chain perturb the binding properties of lipases. Perkins et al.[29] have stressed the suitability of SLFA for use as surrogates for fatty acids. In our case, the differences in the binding constants of the same SLFA in lipases A and B permit one to structurally distinguish lipase A from the rest of the *C. rugosa* family, the value of this constant for lipase A being approximately twice as large as for lipase B.

On the basis of the data in Tables 2 and 3, the differences in the substrate specificities of the *C. rugosa* isolipases may be analyzed in terms of the mobility of the substrate at the binding site and/or the values of the binding constant, both being higher for lipase A (differences in polarity have been ruled out as a factor in this variability). However, the lipolytic activity for the hydrolysis of triolein is higher for lipase B than for lipase A.[18] Assuming that in this reaction the binding strength of oleic acid in the two lipases parallels that of one of the DSA substrates, it is the conformational mobility of the substrate chain which seems to be more important in hydrolysis. Kamiya and Goto[49] have shown that the catalytic activity of *C. rugosa* lipases for different fatty acids largely depends on the binding step, whereas it does not depend on the deacylation step.

C. rugosa lipases exhibit four interdependent binding sites for labeled stearic acids (Table 3). Complexes of the major lipase with different inhibitors and at different molar ratios of lipase to inhibitor suggest the existence, in addition to the aforementioned tunnel, of at least two additional sites for binding two more fatty acyl chains,[48] namely an ovoid crevice above the catalytic site and a more superficial region which might interact with a third fatty acid. The tail of the acid bound to the last site extends into the solvent. While the positions of the first two acid molecules are relatively fixed, the third might adopt several conformations. Grochulski et al.[48] showed that the hydrophobic area surrounding the active site is essential for binding fatty acids to the lipase. Their work demonstrated that while the second inhibitor molecule was covalently bound to the catalytic His 449 group, two superficial His groups were not modified at high concentrations of the inhibitor. Since the binding of SLFA is both highly specific and cooperative (Table 3), it is very likely that the fourth molecule of labeled stearic acid also binds at the superficial region of the hydrophobic pocket of the protein beside the third SLFA molecule.

Access of the first molecule of inhibitor to the tunnel of the protein where the binding takes place is very constrained.[48] Motion of two subdomains of the protein has been suggested to facilitate binding of the acid.[48] The cooperative character of the binding of the labeled acid to these lipases might support this hypothesis. According to the α values (Table 3), undeter-

mined rearrangements of the protein molecule take place as the different binding sites become occupied.

In conclusion, the comparative EPR study of lipase A and lipase B has provided valuable information for characterizing specific molecular binding of substrate analogues in these two lipases and for understanding their different catalytic properties (intrinsic activity and substrate specificity).

Acknowledgment. Financial support from the Spanish CICYT (No. BIO 96-0837) is gratefully aknowledged. In addition, we are grateful to the NATO Scientific Commitee for supporting this work by the award of a fellowship to H.C.

References and Notes

(1) Jensen, R. G.; Dejong, F. A.; Clark, R. M. *Lipids* **1983**, *18*, 239.
(2) Chapus, C.; Rovery, M.; Sarda, L.; Verger, R. *Biochimie* **1988**, *70*, 1223.
(3) Chapus, C.; Semeriva, M.; Bovier-Lapierre, C.; Desnuelle, P. *Biochemistry* **1976**, *15*, 4980.
(4) Brokman, H. L.; Law, J. H.; Kezdy, F. J. *J. Biol. Chem.* **1973**, *248*, 4965.
(5) Entressangles, B., and Desnuelle, P. J. *Biochim. Biophys. Acta* **1974**, *341*, 437.
(6) Bradly, L.; Brzozowski, A. M.; Derewenda, Z. S.; Dodson, E.; Dodson, G.; Tolley, S.; Turkenburg, J. P.; Christiansen, L.; Huge-Hensen, B.; Norskov, L.; Thim, L.; Menge, U. *Nature* **1990**, *343*, 767.
(7) Winkler, F. K.; D′Arcy, A.; Hunziker, W. *Nature* **1990**, *343*, 771.
(8) Schrag, J. D.; Li, Y.; Wu, S.; Cygler, M. *Nature* **1991**, *351*, 761.
(9) Derewenda, U.; Brzozowski, A. M.; Lawson, D. M.; Derewenda, Z. S. *Biochemistry* **1992**, *31*, 1532.
(10) Kawaguchi, Y.; Honda, H. *Nature* **1989**, *341*, 164.
(11) Longhi, S.; Lotti, M.; Fusetti, F.; Brocca, S.; Pizzi, E.; Tramontano, A.; Alberghina, L. *Biochim. Biophys. Acta* **1992**, *1165*, 129.
(12) Lotti, M.; Grandori, R.; Fusetti, F.; Longhi, S.; Brocca, S.; Tramontano. A.; Alberghina, L. *Gene* **1993**, *124*, 45.
(13) Rúa, M. L.; Días-Mauriño, T.; Otero, C.; Ballesteros, A. *Ann. N. Y. Acad. Sci.* **1992**, *672*, 20.
(14) Otero, C.; Rúa, M. L.; Robledo, L. *FEBS Lett.* **1995**, *360*, 202.
(15) Lotti, M.; Tramontano, A.; Longhi, S.; Fusetti, F.; Brocca, S.; Pizzi, E.; Alberghina, L. *Protein Eng.* **1994**, *7*, 531.
(16) Shaw, J. F.; Chang, C. H. *Biotechnol. Lett.* **1989**, *11*, 779.
(17) Veeraragavan, K.; Gibbs, B. F. *Biotechnol. Lett.* **1989**, *11*, 345.
(18) Rúa, M. L.; Diaz-Mauriño, T.; Fernández, V. M.; Otero, C.; Ballesteros, A. *Biochim. Biophys. Acta* **1993**, *1156*, 181.
(19) Grochulski, P.; Li, Y.; Schrag, J. D.; Bouthillier, F.; Smith, P.; Harrison, D.; Rubin, B.; Cygler, M. J. *Biol. Chem.* **1993**, *268*, 12843.
(20) Grochulski, P.; Li, Y.; Schrag, J. D.; Cygler, M. *Prot. Sci.* **1994**, *3*, 82.
(21) Wallach, D. F. H.; Verma, S. P.; Weidekamm, E.; Bieri, V. *Biochim. Biophys. Acta* **1974**, *356*, 68.
(22) Morrisett, J. D.; Pownall, H. J.; Gotto, A. M. J. *J. Biol. Chem.* **1975,** *250*, 2487.
(23) Kuznetsov, A. N.; Ebert, B.; Lassmann, G.; Shapiro, A. *Biochim. Biophys. Acta* **1975**, *446*, 139.
(24) Ruf, H. H.; Gratzl, M. *Biochim. Biophys. Acta* **1976**, *446*, 134.
(25) Soltys, B. J.; Hsia, J. C. *J. Biol. Chem.* **1977**, *253*, 3023.
(26) Soltys, B. J.; Hsia, J. C. *J. Biol. Chem.* **1977**, *253*, 3029.
(27) Rehfeld, S. J.; Eatough, D. J.; Plachy, W. Z. *J. Lipid Res.* **1978**, *19*, 841.
(28) Berde, C. B.; Hudson, B. S.; Simoni, R. D., Sklar, L. A. *J. Biol. Chem.* **1979**, *25*, 391.
(29) Perkins Jr., R. C.; Abumrad, N.; Balasubramanian, K.; Dalton, L. R.; Beth, A.; Park, J. H.; Park, C. R. *Biochemistry* **1982**, *21*, 4059.
(30) Ge, M.; Rananavare, S. B.; Freed, J. H. *Biochim. Biophys. Acta* **1990**, *1036*, 228.
(31) Gantchev, T. G.; Shopova, M. B. *Biochim. Biophys. Acta* **1990**, *1037*, 422.
(32) Narayan, M.; Berliner, L. J. *Biochemistry* **1997**, *37*, 1906.
(33) Cawthern, K. M.; Narayan, M.; Chaudhuri, D.; Permyakov, E. A.; Berliner, L. J. *J. Biol. Chem.* **1997**, *272*, 30812.
(34) Otero, C.; Pérez-Gil, J. Unpublished data.
(35) Otero, C.; Ballesteros, A.; Guisán, J. M. *Appl. Biochem. Biotechnol.* **1988**, *19*, 163.
(36) Schneider, D. J.; Freed, J. H. In *Biological Magnetic Resonance*; Berliner, L. J., Reuben, J., Eds.; Plenum Press: New York, 1989; Chapter 1.
(37) Program Sim 14 A. *QCPE* **1995**, 265.
(38) Schreier, A. A.; Schimmel, P. R. *J. Mol. Biol.* **1974**, *86*, 601.
(39) Scatchard, G. *Ann. N.Y. Acad. Sci.* **1949**, *51*, 660.
(40) Rosenthal, H. E. *Anal. Biochem.* **1967**, *20*, 525.
(41) Jones, T. A.; Zou, J. Y.; Cowan, S. W. *Acta Crystallogr.* **1991**, *A47*, 110.
(42) Lasic, D. D.; Hauser, H. *J. Phys. Chem.* **1985**, *89*, 2648.
(43) Timmins, G. S.; Davies, M. J.; Gilbert, B. C.; Caldararu, H. *J. Chem. Soc., Faraday Trans.* **1994**, *90*, 2643.
(44) Caldararu, H.; Timmins, G. S.; Davies, M. J.; Gilbert, B. C. *J. Chem. Soc., Faraday Trans*. **1996**, *92*, 3151.
(45) McCalley, R. C.; Schimshick, E. J.; McConnell, H. M. *Chem. Phys. Lett.* **1975**, *13*, 115.
(46) Griffith, O. H.; Jost, P. C. In *Spin labeling I*; Berliner, L. J., Ed.; Academic Press: New York, 1976; p 453.
(47) Caldararu, H.; Caragheorgheopol, A.; Vasilescu M.; Dragutan, I.; Lemmetyinen, H. *J. Phys. Chem.* **1994**, *98*, 5320.
(48) Grochulski, P.; Bouthillier, F.; Kazlauskas, R. J.; Serreqi, A. N.; Schrag, J. D.; Ziomek, E.; Cygler, M. *Biochemistry* **1994**, *33*, 3494.
(49) Kamiya, N.; Goto, M. *Biotechnol. Prog.* **1997**, *13*, 488.